Revista de Matemática: Teoría y Aplicaciones 2013 **20**(1) : 1–20
cimpa – ucr issn: 1409-2433

PATTERN EQUATION METHOD FOR THE SOLUTION OF ELECTROMAGNETIC SCATTERING BY AXIALLY-SYMMETRIC PARTICLES WITH COMPLEX ANISOTROPIC SURFACE IMPEDANCE

MÉTODO DE ECUACIÓN POR PATRONES PARA LA SOLUCIÓN DE SCATTERING ELECTROMAGNÉTICO POR PARTÍCULAS AXIALMENTE SIMÉTRICAS CON IMPEDANCIA DE SUPERFICIE ANISOTRÓPICA COMPLEJA

Alexander G. Kyurkchan* Dmitry B. Demin†

Received: 16/Oct/2011; Revised: 10/Nov/2012;
Accepted: 27/Nov/2012

*Moscow Technical University of Communication and Informatics, Aviamotornaya Street 8A, Moscow, 111024, Russia. E-Mail: kyurkchan@yandex.ru, kyurkchan@mtuci2.ru

†Same address as/*Misma dirección que* A.G. Kyurkchan. E-Mail: mbdeminsds@mail.ru

Abstract

The pattern equation method (PEM) has been extended to solve the scattering problems of electromagnetic waves by particles with mixed anisotropic surface impedance. Thus, the anisotropic impedance boundary conditions are imposed on lateral surface of the particle, and isotropic impedance boundary conditions are imposed on end faces of the particle. The method is formulated for axially-symmetric bodies. The scattering characteristics of the bodies with artificially soft and hard lateral surfaces are presented. The comparison of the results with those obtained by other methods is carried out. The analysis of convergence's rate of numerical algorithm of the PEM and accuracy of numerical calculations are presented. Comparison of our data with numerical results obtained earlier by the PEM in absence of an anisotropic impedance is carried out.

Keywords: Scattering problems, pattern equation method, anisotropic impedance, artificial soft and hard surfaces, bodies with the mixed anisotropic surface impedance.

Resumen

El método de la ecuaciones de patrón (PEM) han sido extendidos para resolver problemas de scattering en ondas electromagnéticas por medio de partículas con superficie de impedancia mista anisotrópica. Luego, las condiciones de frontera de impedancia anisotrópica se imponen en la superficie lateral de la partícula, y condiciones de frontera de impedancia isotrópica se imponen en caras finales de la partícula. El método se formula para cuerpos axialmente simétricos. Se presentan las características del scattering de los cuerpos con superficies laterales artificiales suaves y duras. Se lleva a cabo la comparación de los resultados con los que se obtienen con otros métodos. También se presenta el análisis de la tasa de convergencia del algoritmo numérico PEM y la precisión de los cálculos numéricos. Finalmente se hace la comparación de nuestros datos con los resultados numéricos obtenidos antes con el PEM en ausencia de la impedancia anisotrópica.

Palabras clave: Problemas de scattering, método de ecuaciones de patrones, impedancia anisotrópica, superficies artificiales suaves y duras, cuerpos con superficie de impedancia anisotrópica.

Mathematics Subject Classification: 76B15.

1 Introduction

The problem of scattering by impedance bodies is one of the most studied classical problems of electromagnetism.

In the present paper, the diffraction problem for 3D bodies with mixed anisotropic impedance is considered. In this case, on the lateral surface of the scatterer, the full electromagnetic field satisfies to a generalized anisotropic impedance boundary condition in which the surface impedance is represented as a tensor with the components corresponding to appropriate directions of anisotropy. On the remained surface isotropic impedance conditions are imposed. In the case of cylindrical body and the bodies close to them the remained surface represents its top and bottom bases. The solution of those problems can be used for simulating the scattering characteristics of corrugated and chiral structures. In practice, the simplest situation takes place when the directions of anisotropy are specified for bodies of revolution. Therefore, only such bodies will be further considered.

For solving the aforementioned problem, the generalization of the pattern equation method (PEM) has been developed. This method has been earlier applied to solving the problems of electromagnetic waves scattering on the perfectly conducting, impedance, and dielectric scatterers as well as the scatterers coated with several dielectric layers [1-7]. According to [3] (see also [6]), the impedance approach is suitable for modeling the problems of diffraction on bodies with the dielectric absorbing covering, the sizes of which have some lengths of the incident field wave. Recently the algorithm of the PEM has been developed for the solution of scattering problems on scatterers with the anisotropic impedance boundary conditions that are imposed everywhere at the scatterers's surface [8].

The example of bodies with surface anisotropic impedance is a periodic ridge (or corrugated structure) with the grooves filled with a dielectric material. The consideration of such a structure has been made in [9] for the strict electromagnetic statement of the problem.

The numerical algorithm of the PEM is based on the reduction of the original boundary-value problem for Maxwell's equations to an infinite system of linear algebraic equations with respect to the unknown coefficients of the expansion of the scattering pattern (spectral characteristic of the wave field) in terms of vector angular spherical harmonics. The obtained infinite linear system of the algebraic equations is solved by the method of a reduction with certain restrictions on the geometry of the problem, which have been strictly established in [1-4].

The PEM is one of the most effective and universal methods for solving the scattering problems of electromagnetic waves. It has been earlier shown [1-3] that the rate of convergence of the PEM's numerical algorithm is mainly governed by the scatterer size and weekly depends on its geometry. If the scatterer is sphere, this method leads to the obvious analytical solution in the form of infinite Fourier's series over wave spherical harmonics, which coincides with the corresponding solution in the theory of Mie series (see [1, 6], for instance).

In the frames of the boundary-value problem, we carried out a simulation of the scattering problem for a plane wave being incident on axially-symmetric bodies with artificial soft and hard lateral surfaces. The definition of such surfaces in the electromagnetic case has been first introduced by P-S Kildal [10-11]. The description of such surfaces in terms of anisotropic impedance independently from polarization of an incident plane wave was presented more in detail in [8]. Further we study accuracy of the obtained numerical calculations by means of values of the scattering pattern, and also where it was possible, under the optical theorem. We have calculated the some scattering characteristics for finite circular cylinders and superellipsoids. On lateral surface of these scatterers anisotropic impedance boundary conditions were imposed, and the top and bottom bases were either perfectly conducting or caused by some isotropic impedance. Further, we have compared these characteristics with those have been obtained by the PEM for scatterers which surface has been entirely caused by an anisotropic impedance.

2 Problem statement

Consider an electromagnetic wave scattering problem of a primary monochromatic ($e^{i\omega t}$) field $\vec{E}^0$, $\vec{H}^0$ that is incident on an arbitrarily shaped 3D compact body bounded by closed surface S as shown in Figure 1. Let us denote the lateral surface of the body as S_l , and the basis of the cylindrical body (that is the top and bottom faces) as S_b. Then we have: $S = S_l \cup S_b$.

Let the following anisotropic impedance boundary condition be met at surface S:

$$(\vec{n} \times \vec{E})|_{S_l} = \mathbf{Z}[\vec{n} \times (\vec{n} \times \vec{H})]\Big|_{S_l} \tag{1a}$$

$$(\vec{n} \times \vec{E})|_{S_b} = \mathbf{Z}[\vec{n} \times (\vec{n} \times \vec{H})]\Big|_{S_b} \tag{1b}$$

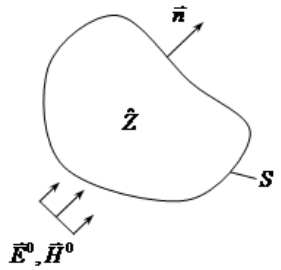

Figure 1: Layout of the problem.

where $\vec{n}$ is the outward unit normal to S; $\mathbf{Z}$ in (1a) is the anisotropic surface impedance that is represented as a tensor:

$$\mathbf{Z} = \begin{bmatrix} Z_l & Z_{l\varphi} \\ Z_{\varphi l} & Z_\varphi \end{bmatrix}, \tag{2}$$

Z_b in (1b) is the scalar impedance of the basis of the cylindrical body; $\vec{E} = \vec{E}^0 + \vec{E}^1$, $\vec{H} = \vec{H}^0 + \vec{H}^1$ is the total field; $\vec{E}^1$, $\vec{H}^1$ is the secondary (diffracted) field, which satisfies the system of homogeneous Maxwell's equations:

$$\bigtriangledown \times \vec{E}^1 = -ik\zeta\vec{H}^1, \bigtriangledown \times \vec{H}^1 = \frac{ik}{\zeta}\vec{E}^1 \tag{3}$$

elsewhere outside S and the Sommerfeld radiation condition at infinity. Here $k = \omega\sqrt{\varepsilon\mu}$ and $\zeta = \sqrt{\mu/\varepsilon}$ are the wave number and the free-space wave impedance, respectively.

The component Z_i of tensor $\mathbf{Z}$ corresponds to the direction of unit vector $\vec{i}_\varphi$, which is tangential to $S_l$and perpendicular to unit vectors $\vec{i}_\varphi$ (unit vector of a spherical coordinate system (r, θ, φ)) and to $\vec{n}$. Let vector $\vec{i}_l$ be equal to $(\vec{i}_\varphi \times \vec{n})$. Thus, vectors $\vec{i}_l$, $\vec{i}_\varphi$, and $\vec{n}$ form a right-hand orthogonal system. It is clear that components Z_l and Z_φ are the surface impedances along the main directions of anisotropy corresponding to vectors $\vec{i}_l$ and $\vec{i}_\varphi$.

Using the expansion of the vector $\vec{E}$ (and similar for $\vec{H}$) in the form

$$\vec{E} = E_\varphi\vec{i}_\varphi + E_l\vec{i}_l + E_n\vec{n},$$

and substituting it into boundary condition (1a), we obtain

$$E_\varphi\vec{i}_l = (Z_lH_l + Z_{l\varphi}H_\varphi)\vec{i}_l + (Z_{\varphi l}H_l + Z_\varphi H_\varphi)\vec{i}_\varphi. \tag{4}$$

If $Z_{l\varphi} = Z_{\varphi l} = 0$, we obtain the following impedance condition:

$$E_\varphi \vec{i}_l - E_l \vec{i}_\varphi = Z_l H_l \vec{i}_l + Z_\varphi H_\varphi \vec{i}_\varphi,$$

which is similar that is resulted in paper [11].

For solving the scattering problem (1)–(3) in the framework of the PEM we used the spherical basis for decomposition the scattering pattern and wave fields. It reduces directly the initial problem to the algebraic system with respect to the unknown coefficients of the pattern expansion in terms of spherical harmonics.

3 Reduction of boundary-value problem to system of algebraic equations

Further, we describe the standard scheme of deriving the numerical algorithm of PEM.

According to papers [1-4], we are going to find the scattering pattern function, that is, the function that defines the dependence of the diffracted field on angles (θ, φ) in spherical coordinates (r, θ, φ) for the far zone $(kr \gg 1)$ where the following asymptotic relations are valid:

$$\begin{aligned} \vec{E}^1 &= \frac{\exp(-ikr)}{r} \vec{F}^E(\theta, \varphi) + O\left(\frac{1}{(kr)^2}\right), \\ \vec{H}^1 &= \frac{\exp(-ikr)}{r} \vec{F}^H(\theta, \varphi) + O\left(\frac{1}{(kr)^2}\right). \end{aligned}$$

Here $\vec{F}^E$ and $\vec{F}^H$ are the scattering patterns for electrical and magnetic fields, respectively.

The basic point of the PEM consists in obtaining the infinite system of algebraic equations with respect to unknown expansion coefficients of the scattering patterns into series in terms of vector angular spherical harmonics [12], which form the orthogonal basis in the spherical coordinates. The series expansions of the scattering patterns have the following form (the details can be found in [1], for instance):

$$\vec{F}^E(\theta, \varphi) = -\sum_{n=1}^{\infty} \sum_{m=-n}^{n} a_{nm} i^n (\vec{i}_r \times \vec{\Phi}_n^m(\theta, \varphi)) - \sum_{n=1}^{\infty} \sum_{m=-n}^{n} b_{nm} i^n \zeta \vec{\Phi}_n^m(\theta, \varphi), \tag{5}$$

$$\vec{F}^H(\theta,\varphi)=\sum_{n=1}^{\infty}\sum_{m=-n}^{n}a_{nm}i^n\frac{1}{\zeta}\vec{\Phi}_n^m(\theta,\varphi)-\sum_{n=1}^{\infty}\sum_{m=-n}^{n}b_{nm}i^n(\vec{i}_r\times\vec{\Phi}_n^m(\theta,\varphi)), \tag{6}$$

where

$$\vec{\Phi}_n^m(\theta,\varphi)=\vec{r}\times\bigtriangledown P_n^m(\cos\theta)\cdot\exp(im\varphi), \tag{7}$$

and a_{nm}, b_{nm} are the unknown expansion coefficients of the scattering patterns that are to be determined. In formulas (5)-(7),$i=\sqrt{-1}$ is imaginary unit, $\vec{i}_r$ is the unit vector in the spherical coordinate system, and $P_n^m(cos\theta)$ are the associated Legendre functions.

Moreover, the wave field $\vec{E}^1$, $\vec{H}^1$ also can be expanded into series of the vector spherical wave functions with respect to unknown coefficients a_{nm}, b_{nm} :

$$\vec{E}^1=\sum_{n=1}^{\infty}\sum_{m=-n}^{n}\{a_{nm}\vec{E}_{nm}^e+b_{nm}\vec{E}_{nm}^h\}, \tag{8}$$

$$\vec{H}^1=\sum_{n=1}^{\infty}\sum_{m=-n}^{n}\{a_{nm}\vec{H}_{nm}^e+b_{nm}\vec{H}_{nm}^h\}, \tag{9}$$

where

$$\begin{aligned}\vec{E}_{nm}^e&=\bigtriangledown\times\bigtriangledown\times(\vec{r}\Psi_{nm})=\vec{H}_{nm}^h,\\ \vec{E}_{nm}^h&=-ik\zeta\bigtriangledown\times(\vec{r}\Psi_{nm})=-\zeta^2\vec{H}_{nm}^e\\ \Psi_{nm}&=h_n^{(2)}(kr)P_n^m(\cos\theta)\exp(im\varphi),\end{aligned} \tag{10}$$

$h_n^{(2)}$ are the spherical Hankel functions of the second kind.

The starting point for the subsequent analysis is representing coefficients a_{nm}, b_{nm} in terms of the boundary values of the wave field (1). By analogy with [2, 8], we use the following integral relations for the field $\vec{E}^1$, $\vec{H}^1$, which can be obtained from the Maxwell's equations (3):

$$\begin{aligned}\vec{E}^1 &= \int_S\frac{\zeta}{ik}[\bigtriangledown\times\bigtriangledown\times(\vec{I}^eG_0)]ds'+\int_{S_l}\mathbf{Z}[\bigtriangledown\times(\vec{I}^mG_0)]ds'\\ &\quad +Z_b\int_{S_b}[\bigtriangledown\times(\vec{I}^mG_0)]ds', \qquad (11)\\ \vec{H}^1 &= \int_{S_b}[\bigtriangledown\times(\vec{I}^eG_0)]ds'-\int_{S_l}\frac{\mathbf{Z}}{ik\zeta}[\bigtriangledown\times\bigtriangledown\times(\vec{I}^mG_0)]ds'\\ &\quad - Z_b\int_{S_b}\frac{1}{ik\zeta}[\bigtriangledown\times\bigtriangledown\times(\vec{I}^mG_0)]ds', \qquad (12)\end{aligned}$$

where

$$\vec{I}^e = (\vec{n}\times\vec{H})\Big|_S;\ \vec{I^m} = \vec{n}\times(\vec{n}\times\vec{H})\Big|_S = (\vec{n}H_n - \vec{H})\Big|_S = -\vec{H}_\tau\Big|_S,$$

$$H_n = \vec{n}\cdot\vec{H}, \tag{13}$$

$G_0 = \dfrac{\exp(-ik|\vec{r}-\vec{r}'|)}{4\pi|\vec{r}-\vec{r}'|}$ is the fundamental solution (the free-space Green function) for the scalar Helmholtz equation in free space, which is decomposed in the following series at $r > r'$:

$$G_0(\vec{r}-\vec{r}') = \frac{k}{4\pi i}\sum_{n=1}^{\infty}\sum_{m=-n}^{n}(2n+1)\frac{(n-m)!}{(n+m)!}\psi_{nm}(\vec{r})\bar{\chi}(\vec{r}'), \tag{14}$$

$$\chi_{nm} = j_n(kr)P_n^m(\cos\theta)\exp(im\varphi). \tag{15}$$

Here j_n are the spherical Bessel functions and $\vec{r}'$ is the position vector of a point on S.

By comparing Eqs.(8)-(9) with (11)-(12), it was established [2] that

$$\begin{aligned} a_{nm} &= -\frac{N_{nm}\zeta}{4\pi}\left\{\int_S \vec{I}^e(r')\cdot\overline{\vec{e}^e_{nm}(r')}ds'\right. \\ &\quad -\int_{S_l}\mathbf{Z}\cdot\vec{I}^m(r')\cdot\overline{\vec{h}^e_{nm}(r')}ds' \\ &\quad \left.-Z_b\int_{S_b}\vec{I}^m(r')\cdot\overline{\vec{h}^e_{nm}(r')}ds'\right\}, \end{aligned} \tag{16}$$

$$\begin{aligned} b_{nm} &= -\frac{N_{nm}}{4\pi\zeta}\left\{\int_S \vec{I}^e(r')\cdot\overline{\vec{e}^h_{nm}(r')}ds'\right. \\ &\quad -\int_{S_l}\mathbf{Z}\cdot\vec{I}^m(r')\cdot\overline{\vec{h}^h_{nm}(r')}ds' \\ &\quad \left.-Z_b\int_{S_b}\vec{I}^m(r')\cdot\overline{\vec{h}^h_{nm}(r')}ds'\right\}, \end{aligned} \tag{17}$$

where

$$\begin{aligned} \vec{e}^e_{nm} &= \bigtriangledown\times\bigtriangledown\times(\vec{r}\chi_{nm}) \\ &= \vec{h}^h_{nm};\ \vec{e}^h_{nm}? - ik\zeta\bigtriangledown\times(\vec{r}\chi_{nm}) \\ &= -\zeta^2\vec{h}^e_{nm};\ N_{nm} = \frac{2n+1}{n(n+1)}\frac{(n-m)!}{(n-m)!}. \end{aligned} \tag{18}$$

Now, using relations (16)–(17) and replacing quantities $\vec{I}^e$ and $\vec{I}^m$ by corresponding expansions of wave fields in view of Eq. (13), we obtain the following infinite system of the linear algebraic equations of PEM

$$\begin{cases} a_{nm} = & a^0_{nm} + \sum_{q=1}^{\infty}\sum_{p=-q}^{q}(G^{11}_{nm,qp}a_{qp} + G^{12}_{nm,qp}b_{qp}), \\ b_{nm} = & b^0_{nm} + \sum_{q=1}^{\infty}\sum_{p=-q}^{q}(G^{21}_{nm,qp}a_{qp} + G^{22}_{nm,qp}b_{qp}) \\ & n = 1, 2, ..., \ |m| \le n, \end{cases} \tag{19}$$

where

$$\begin{cases} a^0_{nm} = & a^{00}_{nm} + a^{\tilde{z}0}_{nm};\ b^0_{nm} = b^{00}_{nm} + b^{\tilde{z}0}_{nm};\ G^{ij}_{nm,qp} = G^{0ij}_{nm,qp} + G^{\tilde{z}ij}_{nm,qp}; \\ i, j = & 1, 2. \end{cases} \tag{20}$$

Here, the additional superscript marked by "0" corresponds to the perfect conductor ($\mathbf{Z} = 0$), and those marked by "$\tilde{z}$" designates the additional terms caused by the anisotropic impedance $\mathbf{Z}$. Coefficients a^0_{nm}, $b^0_{nm}$are determined by the incident wave. These coefficients and the matrix elements $G^{ij}_{nm,qp}$, $i, j = 1, 2$ in Eq. (20) are represented by surface integrals on S as follows:

$$\begin{aligned} a^{00}_{nm} &= -\frac{N_{nm}\zeta}{4\pi}\int_S (\vec{n}\times\vec{H}^0)\cdot\overline{\vec{e}^e_{nm}}ds,\ b^{00}_{nm} \\ &= -\frac{N_{nm}}{4\pi\zeta}\int_S (\vec{n}\times\vec{H}^0)\cdot\overline{\vec{e}^h_{nm}}ds, \\ a^{\tilde{z}0}_{nm} &= -\frac{N_{nm}\zeta}{4\pi}\left\{\int_{S_l}(\mathbf{Z}\vec{H}^0_\tau)\cdot\overline{\vec{h}^e_{nm}}ds + Z_b\int_{S_b}\vec{H}^0_\tau\cdot\overline{\vec{h}^e_{nm}}ds\right\}, \\ b^{\tilde{z}0}_{nm} &= -\frac{N_{nm}}{4\pi\zeta}\left\{\int_{S_l}(\mathbf{Z}\vec{H}^0_\tau)\cdot\overline{\vec{e}^e_{nm}}ds + Z_b\int_{S_b}\vec{H}^0_\tau\cdot\overline{\vec{e}^e_{nm}}ds\right\}; \\ G^{011}_{nm,qp} &= -\frac{N_{nm}\zeta}{4\pi}\int_S (\vec{n}\times\vec{H}^e_{qp})\cdot\overline{\vec{e}^e_{nm}}ds,\ G^{012}_{nm,qp} \\ &= -\frac{N_{nm}\zeta}{4\pi}\int_S (\vec{n}\times\vec{H}^h_{qp})\cdot\overline{\vec{e}^e_{nm}}ds, \\ G^{021}_{nm,qp} &= -\frac{N_{nm}\zeta}{4\pi}\int_S (\vec{n}\times\vec{H}^e_{qp})\cdot\overline{\vec{h}^e_{nm}}ds,\ G^{022}_{nm,qp} \\ &= -\frac{N_{nm}\zeta}{4\pi}\int_S (\vec{n}\times\vec{H}^h_{qp})\cdot\overline{\vec{h}^e_{nm}}ds, \end{aligned} \tag{21}$$

$$
\begin{aligned}
G^{\tilde{z}11}_{nm,qp} &= -\frac{N_{nm}\zeta}{4\pi}\left\{\int_{S_l}\mathbf{Z}[\vec{n}\times(\vec{n}\times\vec{H}^e_{qp})]\cdot\overline{\vec{h}^e_{nm}}ds\right. \\
&\quad \left.+Z_b\int_{S_b}[\vec{n}\times(\vec{n}\times\vec{H}^e_{qp})]\cdot\overline{\vec{h}^e_{nm}}ds\right\}, \qquad (22)\\
G^{\tilde{z}12}_{nm,qp} &= -\frac{N_{nm}\zeta}{4\pi}\left\{\int_{S_l}\mathbf{Z}[\vec{n}\times(\vec{n}\times\vec{H}^h_{qp})]\cdot\overline{\vec{h}^e_{nm}}ds\right. \\
&\quad \left.+Z_b\int_{S_b}[\vec{n}\times(\vec{n}\times\vec{H}^h_{qp})]\cdot\overline{\vec{h}^e_{nm}}ds\right\}, \\
G^{\tilde{z}21}_{nm,qp} &= -\frac{N_{nm}}{4\pi\zeta}\left\{\int_{S_l}\mathbf{Z}[\vec{n}\times(\vec{n}\times\vec{H}^e_{qp})]\cdot\overline{\vec{e}^e_{nm}}ds\right. \\
&\quad \left.+Z_b\int_{S_b}[\vec{n}\times(\vec{n}\times\vec{H}^e_{qp})]\cdot\overline{\vec{e}^e_{nm}}ds\right\}, \\
G^{\tilde{z}22}_{nm,qp} &= -\frac{N_{nm}}{4\pi\zeta}\left\{\int_{S_l}\mathbf{Z}[\vec{n}\times(\vec{n}\times\vec{H}^h_{qp})]\cdot\overline{\vec{e}^e_{nm}}ds\right. \\
&\quad \left.+Z_b\int_{S_b}[\vec{n}\times(\vec{n}\times\vec{H}^h_{qp})]\cdot\overline{\vec{e}^e_{nm}}ds\right\}.
\end{aligned}
$$

The system of the linear algebraic equations of PEM (19) can be used for calculating the scattering characteristics of arbitrarily shaped scatterers, which are not axially symmetric. When the scatterer is an axially symmetric object (body of revolution), i.e. the surface equation takes the form $\rho(\theta,\varphi=\rho(\theta)$, the algebraic system (19) considerably simplifies and can be written as

$$
\begin{cases}
a_{nm}=a^0_{nm}+\sum_{q=|m|}^{N}(G^{11}_{nm,qm}a_{qm}+G^{12}_{nm,qm}b_{qm}),\\
n=1,2,...,N;\ |m|\le n,\\
b_{nm}=b^0_{nm}+\sum_{q=|m|}^{N}(G^{21}_{nm,qm}a_{qm}+G^{22}_{nm,qm}b_{qm})
\end{cases} \qquad (23)
$$

where N is the upper limit of summation in Eq. (16), that is, the maximal number of harmonic functions in series (5)-(6). Matrix elements in (23) are expressed in terms of single integrals.

To justify the applicability of the method of reducing to the obtained infinite system (19), the matrix elements and the right-hand part of the system can be estimated for large values of n and q. Such an estimation is similar to that earlier performed for the numerical algorithm of PEM (see, for example, [1-4]). That approach allows us to specify rigorous limitations on the geometry of the scatterers. If the incident field is a

plane wave, the method of reducing is valid if the scatterer belongs to a class of weakly non-convex bodies [1-4]. In particular, this class contains all convex bodies.

Note that, for perfectly conducting bodies of revolution, the algebraic system similar to (23), seems to be first obtained in [13] for the case when the scatterer belongs to a class of so-called Rayleigh bodies (see [14], for instance). However, the PEM has been independently developed [15] on the basis of the strict integral-operator equation with respect to the scattering pattern of a body, and, as it was mentioned above, the PEM is applicable to considerably wider class of scatterers rather than the Rayleigh bodies.

4 Numerical results

In this section, we present some results of calculating of the scattering characteristics for different axially symmetric cylindrical scatterers at whose surfaces the mixed impedance boundary conditions are fulfilled. The z-axis was chosen as the symmetry axis of the scatterers. In all examples, the incident field is a plane unit wave.

The aim of our study is to compute the scattering characteristics for scatterers with artificially soft and hard lateral surfaces.

In [11], the definition of the artificially soft and hard surfaces in an electromagnetic case has been introduced by using the special values of anisotropic impedance. This impedance corresponds to some corrugated structure of surface S with grooves, the edges of which are parallel to either vector $\vec{i}_\varphi$ or vector $\vec{i}_l$. In the same paper, the values of anisotropic impedance are obtained for surfaces that are polarization-independently soft and hard. Generally, those surfaces are artificially soft and hard. It was established (see Eq. (15) in [11]) that, independently of the field polarization, the components of $\mathbf{Z}$ corresponding to the artificially soft surface take the following values

$$|Z_\varphi| = \infty, \ Z_l = 0, \ Z_{l\varphi} = Z_{\varphi l} = 0. \tag{24}$$

Moreover, the direction of vector $\vec{i}_l$ corresponds to the direction of wave propagation along surface S, and vector $\vec{i}_\varphi$ (transverse direction) is perpendicular to the plane of incidence of the wave and to the direction of wave propagation (the direction of vector $\vec{i}_\varphi$ corresponds to that of the grooves).

Similarly, the artificially hard surface can be defined by the following values of the components of anisotropic impedance $\mathbf{Z}$ (see Eq.(17) in [11]):

$$|Z_l| = \infty,\ Z_\varphi = 0,\ Z_{l\varphi} = Z_{\varphi l} = 0. \tag{25}$$

In [8] it was already noticed that the artificially soft surface is a surface with ideal mixed conductivity along the direction $\vec{i}_\varphi$, and, in the same way, the artificially hard surface is a surface with ideal mixed conductivity along the direction $\vec{i}_l$. Thus, the artificially soft scatterer, in general case, should not support of a surface wave. In [9], the question is in detail analyzed about what properties of hard surfaces, in terms of the sizes of grooves, and what properties of materials of a covering of corrugated structures should be.

The scattering problem was considered for the plane wave with circular polarization in the form

$$\vec{E}^0 = (\vec{i}_x cos\theta_0 + \vec{i}_z \sin\theta_0 + \vec{i}_y(\pm i)) \exp(-ikr(-\sin\theta\sin\theta_0\cos\varphi + \cos\theta\cos\theta_0)),$$

$$\vec{H}^0 = \frac{\mp i}{\zeta} \cdot \vec{E}^0. \tag{26}$$

The scatterers were cylindrical bodies, such as a finite circular cylinder and a superellipsoid. In Eq. (26), $\vec{i}_x$ and $\vec{i}_y$ are the unit vectors in Cartesian coordinate system, and the super- and subscripts mean the right and left polarization, respectively. The surface of a superellipsoid in Cartesian coordinate system is defined by equation

$$\frac{x^{2m} + y^{2m}}{a^{2m}} + \frac{z^{2m}}{c^{2m}} = 1 \tag{27}$$

where m is the coefficient of roundedness. The sizes of circular cylinder are as follows: $ka = 1$(a is a radius of the basis of the cylinder), $kh = 10$ (h is the height of the cylinder), and the parameters of the superellipsoid are specified as $ka = 1$, $kc = 5$, and $m = 8$ (the sizes of the superellipsoid correspond to the sizes of the cylinder). Figures 2-7 show the scattering patterns of the electric field (quantities $F^E_\theta(\theta,\varphi)$ and $F^E_\varphi(\theta,\varphi)$) in two half-planes: $\varphi = 0$ (E-plane), and $\varphi = \pi/2$ (H-plane), respectively. In these planes angle θ changes from 0 to 180 degrees. In Figs. 2-3, curves 1 and 2 correspond to the cylinder and superellipsoid with $\mathbf{Z} = 0$, $Z_b = \zeta$ (matched impedance), and curves 3 correspond to the perfectly conducting cylinder ($\mathbf{Z}$ and $Z_b = 0$). In Figs. 4-5, curves 1 and 2 correspond to the cylinder and superellipsoid with $Z_l = 1000\zeta$, $Z_\varphi = 0$ at S_l (hard surface)

and $Z_b = \zeta$ at S_b, and curves 3 correspond to the superellipsoid with the artificially hard lateral surface ($Z_l = 1000\zeta$, $Z_\varphi = 0$, $Z_b = 0$). By analogy, the curves 1 and 2 in Figs. 6-7 correspond to the cylinder and superellipsoid with $Z_l = 0$, $Z_\varphi = 1000\zeta$ (soft surface) at S_l and $Z_b = \zeta$ at S_b, and curves 3 correspond to the superellipsoid with the artificially soft lateral surface ($Z_l = 0$, $Z_\varphi = 1000\zeta$, $Z_b = 0$), respectively. In our calculations, the number 1000ζ replaces infinity in Eqs. (24) and (25), and N is equal to 17-20 (that is, N equals to approximately the height of cylinder). In all calculations, 3-4 correct significant digits in the values of the scattering pattern are obtained. It can be seen From Figs. 6-7 that the scattering patterns for all the scatterers are almost identical in both half-planes but it is not true for artificially hard particles (Figs.4-5). In addition, Fig.6-7 clearly show that the scattering pattern of the superellipsoid with mixed impedance weakly differs from the pattern of the soft superellipsoid in both half-planes. The similar situation is also exhibited by Figs.4-5.

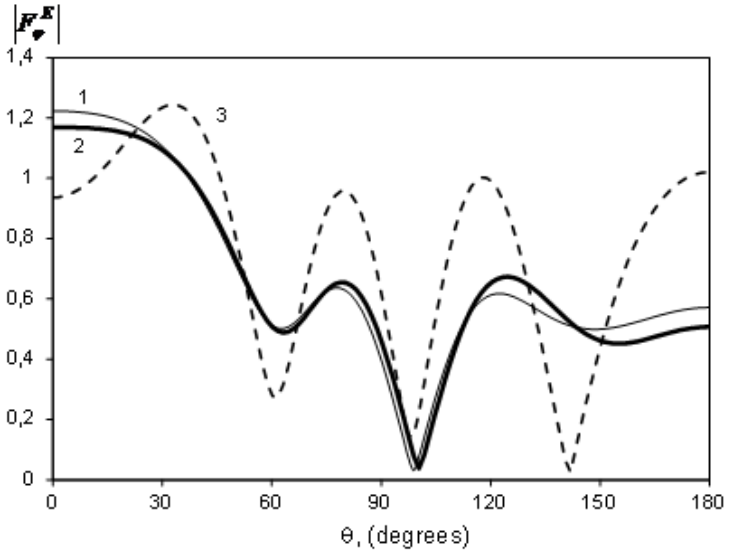

Figure 2: Scattering patterns for the cylinder and superellipsoid (E-plane). Aaxial incidence of a plane wave, perfectly conducting lateral surface.

For comparison, Figs. 8-10 show the scattering patterns for the cylinder and superellipsoid of the same sizes as in Figs. 2-7 but the plane wave is incident perpendicularly to a symmetry axis. Each pattern corresponds

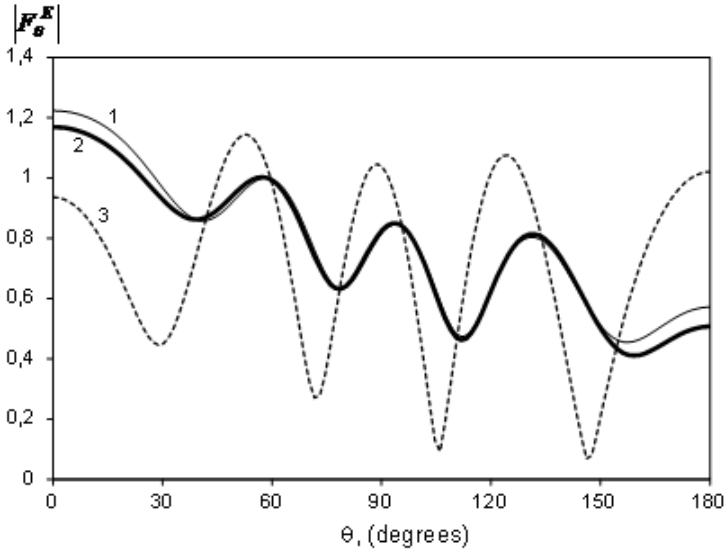

Figure 3: Scattering patterns for the cylinder and superellipsoid (H-plane), Aaxial incidence of a plane wave, perfectly conducting lateral surface.

to plane $\varphi = [0, \pi]$, so as angle θ varies from 0 to 360 degrees. Curves 1 and 2 correspond to the cylinder and superellipsoid, and curves 3 correspond to the superellipsoid with $Z_b = 0$. The following values are specified: $\mathbf{Z} = 0$ and $Z_b = \zeta$ at S_l in Fig.8, $Z_l = 1000\zeta$ and $Z_\varphi = 0$ in Fig.9, with $Z_b = \zeta$, and $Z_l = 0$, $Z_\varphi = 1000\zeta$ at S_l in Fig.10, also with $Z_b = \zeta$. In that case, it can be seen that the scattering patterns shown in all the figures are almost close to each other. It means that the value of impedance Z_b at face surfaces weakly influences the changes in the patterns.

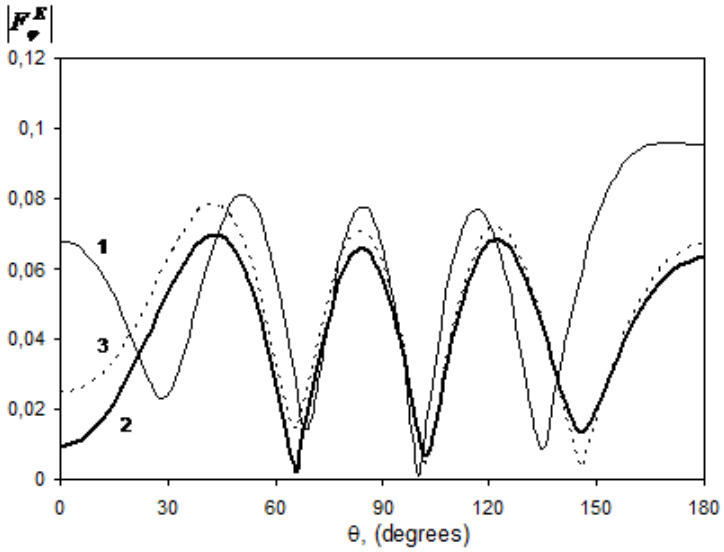

Figure 4: Scattering patterns for the cylinder and superellipsoid (E-plane). Axial incidence of a plane wave, artificially hard lateral surface.

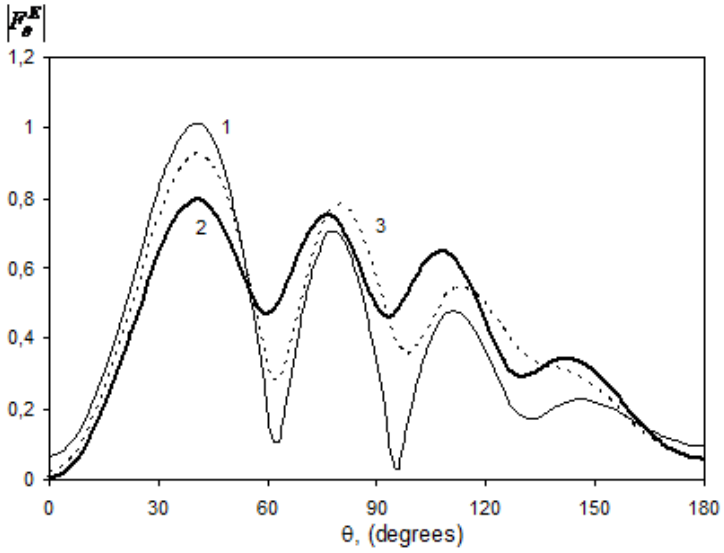

Figure 5: Scattering patterns for the cylinder and superellipsoid (H-plane). Axial incidence of a plane wave, artificially hard lateral surface.

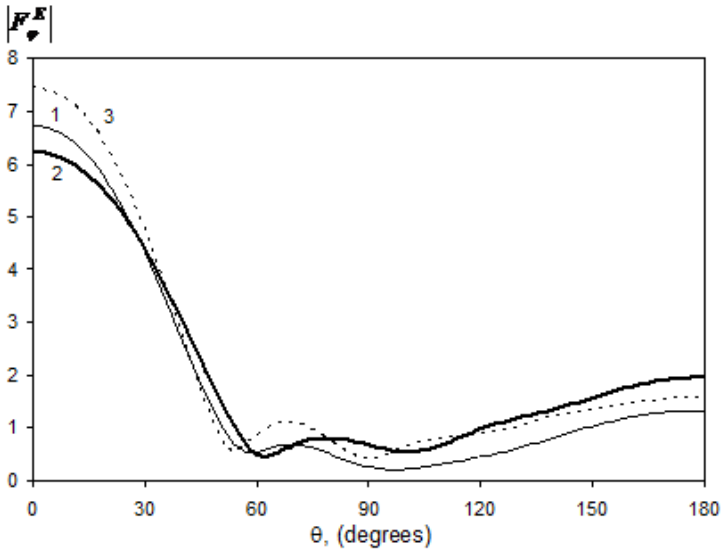

Figure 6: Scattering patterns for the cylinder and superellipsoid (E-plane). Axial incidence of a plane wave, artificially soft lateral surface.

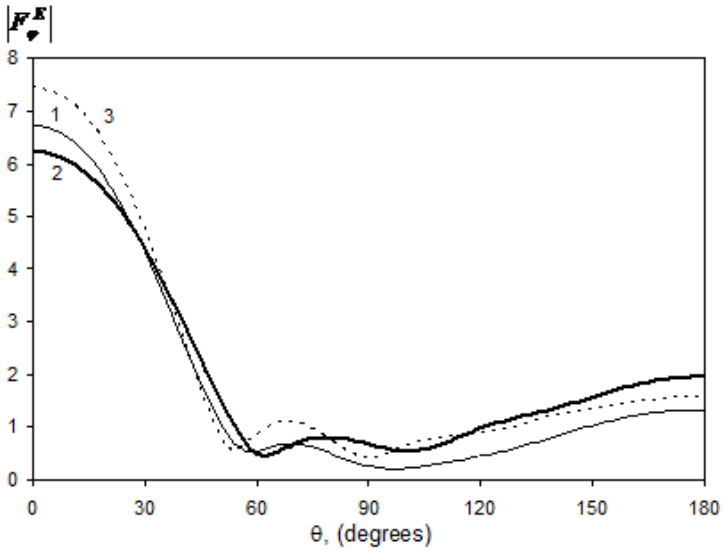

Figure 7: Scattering patterns for the cylinder and superellipsoid (H-plane). Axial incidence of a plane wave, artificially soft lateral surface.

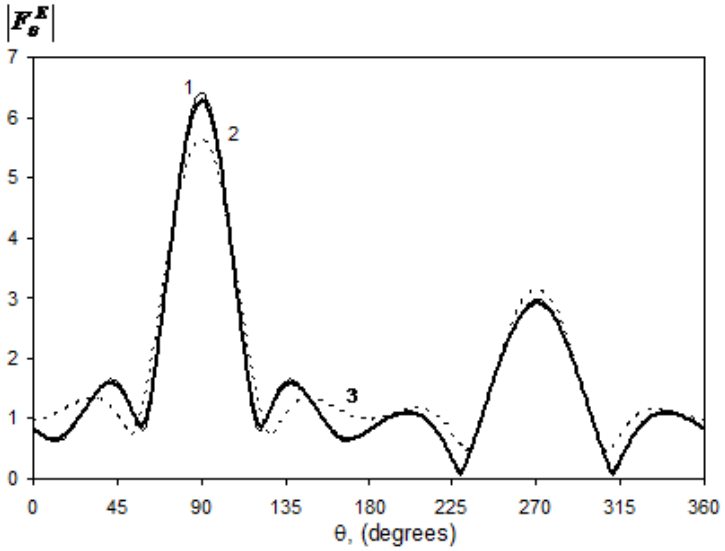

Figure 8: Scattering patterns for the cylinder and superellipsoid (E-plane). Perpendicular incidence of a plane wave, perfectly conducting lateral surface.

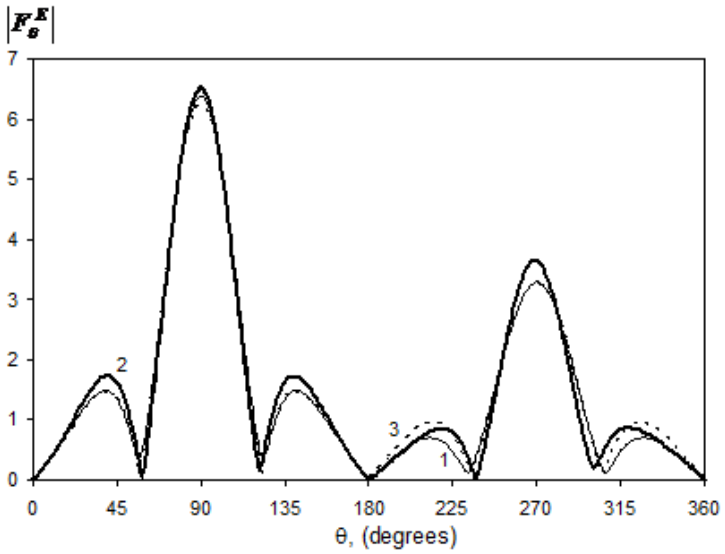

Figure 9: Scattering patterns for the cylinder and superellipsoid (E-plane). Perpendicular incidence of a plane wave, artificially hard lateral surface.

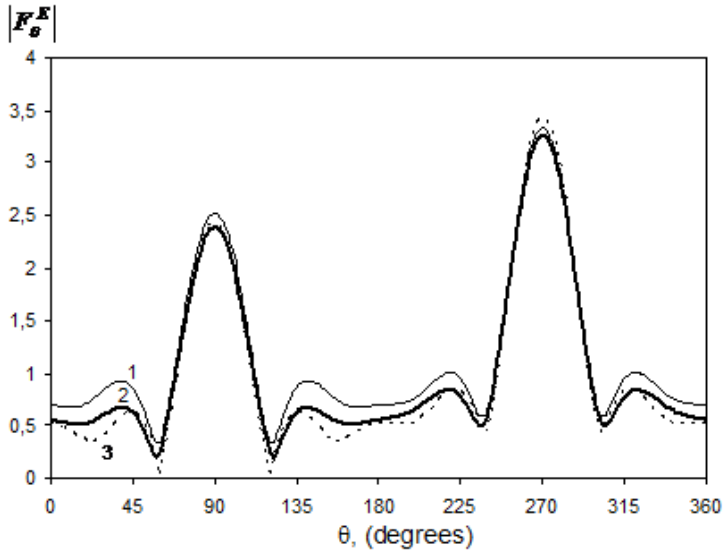

Figure 10: Scattering patterns for the cylinder and superellipsoid (E-plane). Perpendicular incidence of a plane wave, artificially soft lateral surface.

In all the considered examples, the validity of the optical theorem with accuracy not less than 0.001 has been confirmed. According to the optical theorem, the integral scattering cross-section P_S for nonabsorbing scatterers is proportional to the imaginary part of the quantity of the scattering pattern for electrical field P_{S2} in the direction of incidence of the initial plane wave. According to the shown figures, the following results were obtained for superellipsoid with the artificially hard lateral surface:

$$P_S \approx 0,07472,\ P_{s2} \approx 0,07488,$$

where

$$P_S = \frac{1}{2\zeta}\int_0^{2\pi}\int_0^{\pi}\left|\vec{F}^E(\theta,\varphi)\right|^2 \sin\theta d\theta d\varphi, \tag{28}$$

$$P_{S2} = \frac{2\pi}{\zeta} Im\left(\overline{\vec{F}^E}\cdot\vec{g}(\theta_0,\varphi_0)\right),\ \vec{E}^0 = \vec{g}\cdot e^{-i\vec{k}\vec{r}}. \tag{29}$$

5 Conclusions

We demonstrated that impedance conditions with anisotropic impedance are applicable to simulating the scattering characteristics of particles with

mixed anisotropic surface impedance. The results indicate that the PEM is efficient to solve these complicated problems. This approach will be extended to the solution of the electromagnetic wave scattering problems by group of bodies with anisotropic surface impedance.

Acknowledgments

This work was supported by Russian Foundation for Basic Research, Project no. 09-02-00126.

References

[1] Kyurkchan, A.G. (2000) "Solution of vector scattering problems by the pattern equation method", *Journ Comm Tech and Electron* **45**: 970–975.

[2] Kyurkchan, A.G.; Demin. D.B. (2002) "Electromagnetic wave diffraction from impedance scatterers with piecewise–smooth boundaries", *Journ Comm Tech and Electron* **47**: 856–863.

[3] Kyurkchan, A.G.; Demin. D.B. (2004) "Simulation of wave scattering by bodies with an absorbing coating and Black Bodies", *Technical Physics* **49**: 165–173.

[4] Kyurkchan, A.G.; Demin. D.B. (2004) "Pattern equation method for solving problems of diffraction of electromagnetic waves by axially dielectric scatterers", *JQSRT* **89**: 237–255.

[5] Kyurkchan, A.G.; Demin. D.B.; Orlova, N.I. (2007) "Solution of scattering problems of electromagnetic waves from objects with dielectric covering using pattern equation method", *Journal of Commun. Techn. and Electron* **52**: 131–40.

[6] Kyurkchan, A.G.; Demin. D.B.; Orlova, N.I. (2007) "Solution based on the pattern equation method for scattering of electromagnetic waves by objects coated with dielectric materials", *JQSRT* **106**: 192–202.

[7] Kyurkchan, A.G.; Demin. D.B. (2009) "Solution of problem of electromagnetic waves scattering on inhomogeneously layered scatterers using pattern equation method", *JQSRT 110*: 1345–1355.

[8] Kyurkchan, A.G.; Demin. D.B. (2011) "Solution of problems of electromagnetic wave scattering by bodies with an anisotropic impedance with the help of the pattern equation method", *Journal of Commun. Techn. and Electron* **56**: 134–141.

[9] Kyurkchan, A.G. (1999) "Excitation of a periodic ribbed structure possessing the properties of an artificially hard surface by a thread of current", *Journal of Commun. Techn. and Electron.* **44**: 731–737.

[10] Kildal, P.-S. (1988) "Definition of artificially soft and hard surfaces for electromagnetic waves", *Electron. Lett.* **24**(3): 168–170.

[11] Kildal, P.-S. (1990) "Artificially soft and hard surfaces in electromagnetics", *IEEE Transactions on Antennas and Propagation* **38**(10): 1537–1544.

[12] Papas, C.H. (1965) *Theory of Electromagnetic Wave Propagation.* McGraw–Hill, New York.

[13] Hizal, A.; Marincic, A. (1970) "New rigorous formulation of electromagnetic scattering from perfectly conducting bodies of arbitrary shape", *Proc. IEEE* **117**(8): 1639–1647.

[14] Millar, R.F.; Burrows, M.L. (1969) "Rayleigh hypothesis in scattering problems", *Electron. Lett.* **5**: 416–418.

[15] Kyurkchan, A.G. (1992) "A new integral equation in the diffraction theory", *Soviet Physics Doklady* **37**(7): 338–340.